CLEAR

SWMF
SPACE WEATHER MODELING FRAMEWORK

SWORD

Going Beyond MHD: Advances in Space Environment Modeling

Tamas Gombosi
with
Spiro Antiochos, Xiaohang Chen, Bart van der Holst, Zhenguang Huang, Xianzhe Jia, Ward Manchester, Tuija Pulkkinen, Nishtha Sachdeva, Igor Sokolov, Judit Szente, Gabor Toth, Dan Welling, Lulu Zhao, Shasha Zou
+ Weihao Liu, Xianyu Liu, and Elizabeth Wraback

ISSS-15
Garching bei München, Germany
August 1–9, 2024

Space Environment in a Nutshell

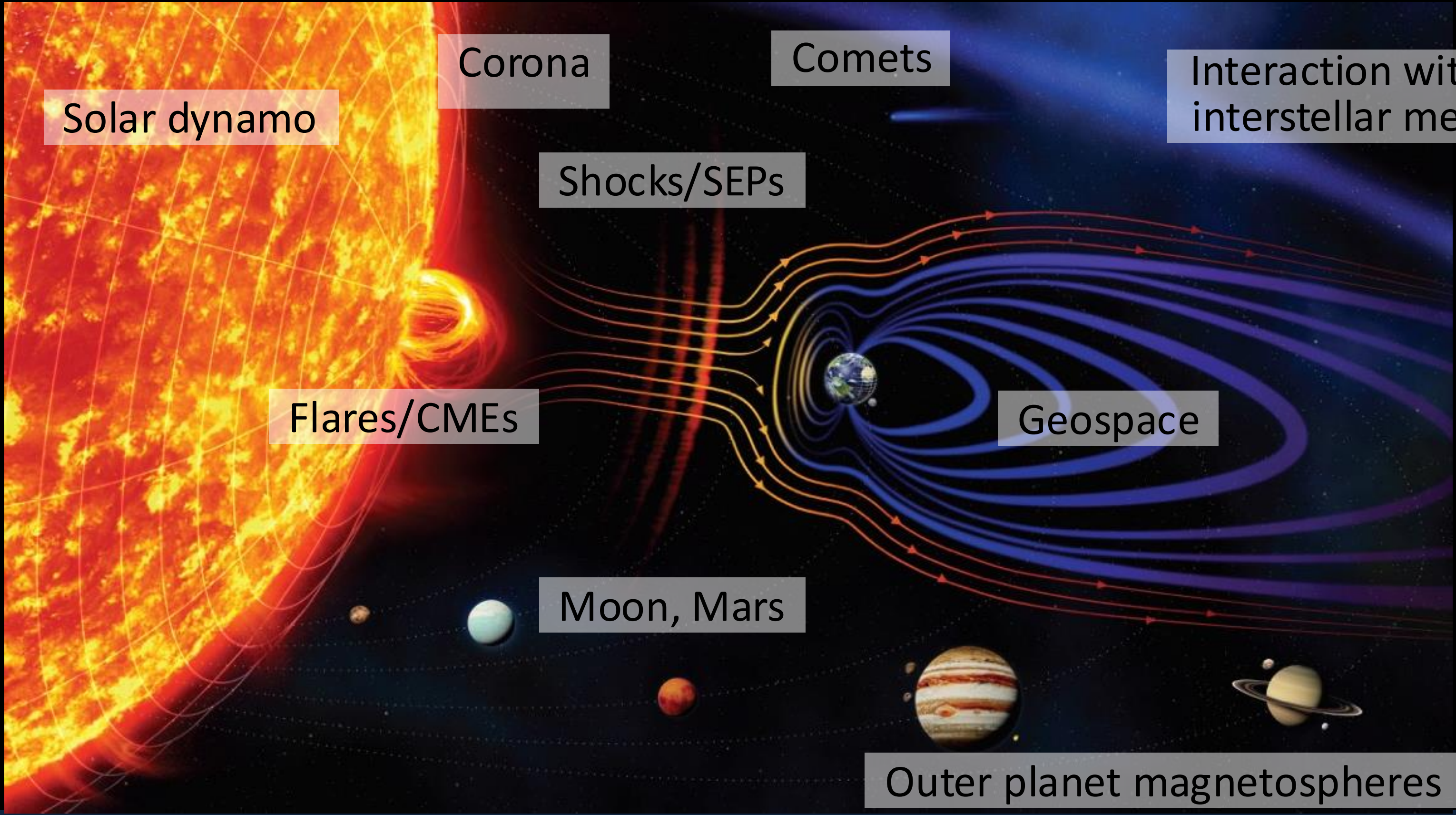

Solar dynamo

Corona

Comets

Interaction with the interstellar medium

Shocks/SEPs

Flares/CMEs

Geospace

Moon, Mars

Outer planet magnetospheres

Typical Space Weather Scale Ratios

	Chromosphere	Transition region	Solar wind (1AU)	Magnetosphere	Plasmasphere	Ionosphere
δ_e/λ_D	10^3	10^2	3×10^2	2×10^1	10^3	3×10^3
r_e/λ_D	10^4	10^3	3×10^2	4×10^2	10^0	10^1
δ_p/λ_D	3×10^4	3×10^3	10^4	7×10^2	3×10^4	10^5
r_p/λ_D	5×10^5	5×10^4	10^4	2×10^4	5×10^1	2×10^2
System size/λ_D	10^{12}	10^8	10^{10}	10^7	10^5	10^9

PiC, Vlasov

Gyrokinetics

Hybrid

MHD, XMHD

Tamas I. Gombosi
tamas@umich.edu
https://tamas.engin.umich.edu

Large-Scale Space Environment Models

Brief History

- Early 1980s: First 3D ideal MHD magnetosphere simulations (UCLA, NRL)
- Mid 1980s: I-M coupling via current closure in a height-integrated ionosphere (NRL)
- Late 1990s:
  - Massively parallel 3D AMR global MHD code for space plasmas with good scaling (Michigan)
  - First 3D global MHD model for the solar corona at SAIC (today PSI)
- Early 2000s:
  - ENLIL, a 3D solar wind wind model (r>0.1AU) developed by Odstrčil
  - Coupling frameworks developed (SWMF/Michigan, CISM)
- Late 2000s:
  - Multifluid, anisotropic and Hall MHD (SWMF/Michigan, LFM)
- Mid-2010s:
  - MHD w. embedded PiC (UCLA/one-way coupling, Michigan/two-way coupling)
  - Integrated solar corona & SEP model (UNH w. PSI)
- Late 2010s:
  - 2D/3D hybrid magnetosphere model (VLASIATOR)
- Early 2020s:
  - MHD with adaptively embedded 2-way coupled PiC (SWMFMichigan)

State of the Art (probably incomplete)

- Global Geospace Models
  - SWMF/Geospace (Michigan)
  - MAGE/GAMERA (under development)
  - OpenGGCM, GUMICS, VLASIATOR
- Physics-based 3D solar corona models (1-20$R_\odot$)
  - MAS/CORHEL (PSI)
  - Usmanov
  - SWMF/AWSoM (Michigan)
  - HelioCubed (UAH)
- Inner heliosphere models (0.1-10AU)
  - ENLIL
  - SWMF/AWSoM (Michigan)
  - CORHEL (PSI)
  - Usmanov
  - Euhforia (Leuven)
  - GAMERA-Helio
  - HelioCubed (UAH)
- Outer heliosphere models
  - SWMF/OH (Michigan)
  - MS-FLUKSS (UAH)
  - Moscow model
- Integrated solar wind – CME – SEP models
  - EMMREM (UAH w.PSI)
  - SWMF/AWSoM/PARMISAN (Michigan)
  - Euhforia-Paradise (Leuven)

Physics-Based Modeling Requirements

- Space environment is inherently multiphysics ⇨ adaptive physics is needed
- Simulation speed is important ⇨ need to forecast the future, not the past
- Space environment is inherently multiscale ⇨ from Debye length to the size of the heliosphere (mesoscale is just one element)
- Multiple timescales must be resolved ⇨ from plasma periods to solar cycles
- To meet these expectations the Space Weather Modeling Framework (SWMF) has been developed over the last quarter of century

Basic Physics: Single-Fluid Ideal MHD

$$\partial_t \rho + (\mathbf{u}\cdot\nabla)\,\rho + \rho\,(\nabla\cdot\mathbf{u}) = 0$$

$$\rho\,\partial_t \mathbf{u} + \rho\,(\mathbf{u}\cdot\nabla)\,\mathbf{u} + \nabla p - \mathbf{j}\times\mathbf{B} = 0$$

$$\partial_t p + (\mathbf{u}\cdot\nabla)\,p + \tfrac{5}{3}p\,(\nabla\cdot\mathbf{u}) = 0$$

$$\partial_t \mathbf{B} - \nabla\times(\mathbf{u}\times\mathbf{B}) = \cancel{\eta_m \nabla^2 \mathbf{B}}$$

$$\mu_0 \mathbf{j} = \nabla\times\mathbf{B}$$

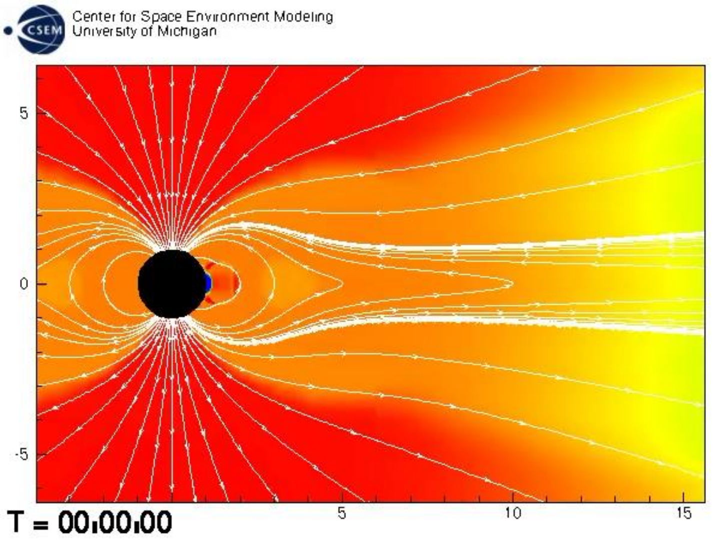

- Even though ideal MHD neglects all dissipation and diffusion processes, discretization ALWAYS introduces them into any numerical solution
- This is the reason for reconnection in ideal MHD codes
- This is a blessing and a curse!

XMHD (multifluid, Hall, anisotropic) I.

- Generalized Ohm’s law:

$$\mathbf{E} = \underbrace{-\mathbf{u}_+ \times \mathbf{B}}_{\text{motional } \mathbf{E} \text{ field}} + \underbrace{\frac{\mathbf{j}}{e\,n_e} \times \mathbf{B}}_{\text{Hall term}} - \underbrace{\frac{\nabla p_e}{e\,n_e}}_{\text{ambipolar term}} + \underbrace{\cancel{\sum_{t=\text{all}} \bar{\nu}_{et} \frac{m_e}{e} (\mathbf{u}_t - \mathbf{u}_+)} - \overbrace{\frac{\bar{\nu}_e\, m_e}{e^2\, n_e}}^{1/\sigma_0} \mathbf{j}}_{\text{resistive term}}$$

- Electron equations (no ionization/recombination):

$$n_e = \sum_{s=\text{ions}} Z_s n_s; \qquad \mathbf{u}_+ = \sum_{s=\text{ions}} \frac{Z_s n_s}{n_e} \mathbf{u}_s$$

charge averaged ion velocity

$$\mathbf{u}_e = \mathbf{u}_+ - \frac{1}{e n_e} \mathbf{j}$$

Hall velocity

heat exchange

$$\partial_t p_e + (\mathbf{u}_e \cdot \nabla) p_e + \tfrac{5}{3} p_e (\nabla \cdot \mathbf{u}_e) + \tfrac{2}{3} \nabla \cdot \mathbf{h}_e = \sum_{t=i/n} 2 \bar{\nu}_{et} m_e n_e \left[\frac{k_B}{m_t} (T_t - T_e) + \tfrac{1}{3} (\mathbf{u}_t - \mathbf{u}_e)^2 \right]$$

heat conduction

frictional heating

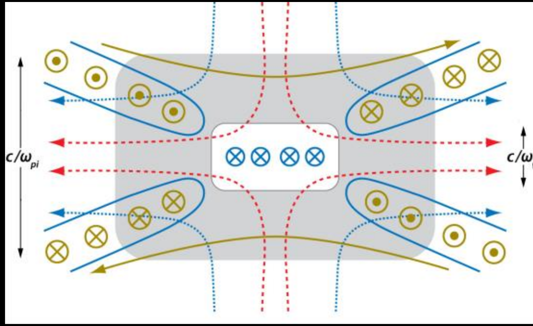

XMHD (multifluid, Hall, anisotropic) II.

$$\partial_t \rho_s + (\mathbf{u}_s \cdot \boldsymbol{\nabla})\rho_s + \rho_s(\boldsymbol{\nabla}\cdot\mathbf{u}_s) = 0$$

$$\partial_t(\rho_s\mathbf{u}_s) + \boldsymbol{\nabla}\cdot\left[\rho_s\mathbf{u}_s\mathbf{u}_s + \left(p_{s_\perp} + \overbrace{\frac{Z_s n_s}{n_e}}^{\text{ion fraction}} p_{e_\perp}\right) I\right] - Z_s e\, n_s \Big[\overbrace{(\mathbf{u}_s - \mathbf{u}_+)\times\mathbf{B}}^{\text{ion drift E field}} + \overbrace{\eta_e \mathbf{j}}^{\text{current dissipation}}\Big] =$$

$$- B\nabla_\parallel \left(\underbrace{\frac{p_{s_\parallel} - p_{s_\perp}}{B}\mathbf{b}}_{\text{adiabatic focusing}}\right) - \frac{Z_s n_s}{n_e} B\nabla_\parallel\left(\frac{p_{e_\parallel} - p_{e_\perp}}{B}\mathbf{b}\right) + \underbrace{\sum_{\mathrm{t=e/i/n}} \bar{\nu}_{st}\rho_s(\mathbf{u}_t - \mathbf{u}_s)}_{\text{friction}}$$

$$\frac{\partial p_{s_\parallel}}{\partial t} + (\mathbf{u}_s\cdot\nabla)p_{s_\parallel} + p_{s_\parallel}(\nabla\cdot\mathbf{u}_s) + 2p_{s_\parallel}\mathbf{b}\cdot\nabla_\parallel\mathbf{u}_s + \nabla_\parallel h_{s_\parallel} = \overbrace{\frac{h_{s_\parallel} - 3h_{s_\perp}}{B}\nabla_\parallel B}^{\text{adiabatic focusing}}$$

$$\underbrace{- \tfrac{2}{3}\left(p_{s_\parallel} - p_{s_\perp}\right)\sum_{\mathrm{t=e/i/n}}\frac{m_s + m_t}{m_t}\bar{\nu}_{st}}_{\text{collisional isotropization}} + \sum_{\mathrm{t=e/i/n}}\bar{\nu}_{st}\frac{m_s n_s}{m_s + m_t}\left[\underbrace{2k_{\mathrm{B}}(T_t - T_s)}_{\text{heat exchange}} + \underbrace{\tfrac{1}{3}m_t(\mathbf{u}_t - \mathbf{u}_s)^2 + m_t\left(u_{t_\parallel} - u_{s_\parallel}\right)^2}_{\text{frictional heating}}\right]$$

$$\frac{\partial p_{s_\perp}}{\partial t} + (\mathbf{u}_s\cdot\nabla)p_{s_\perp} + 2p_{s_\perp}(\nabla\cdot\mathbf{u}_s) - p_{s_\perp}\mathbf{b}\cdot\nabla_\parallel\mathbf{u}_s + \nabla_\parallel h_{s_\perp} = \overbrace{\frac{5h_{s_\perp}}{2B}\nabla_\parallel B}^{\text{adiabatic focusing}}$$

$$\underbrace{+ \tfrac{1}{3}\left(p_{s_\parallel} - p_{s_\perp}\right)\sum_{\mathrm{t=e/i/n}}\frac{m_s + m_t}{m_t}\bar{\nu}_{st}}_{\text{collisional isotropization}} + \sum_{\mathrm{t=e/i/n}}\bar{\nu}_{st}\frac{m_s n_s}{m_s + m_t}\Big[\underbrace{2k_{\mathrm{B}}(T_t - T_s)}_{\text{heat exchange}} + \underbrace{\tfrac{1}{3}m_t(\mathbf{u}_t - \mathbf{u}_s)^2 + \tfrac{1}{2}m_t\left(\mathbf{u}_{t_\perp} - \mathbf{u}_{s_\perp}\right)^2}_{\text{frictional heating}}$$

Tamas I. Gombosi
tamas@umich.edu
https://tamas.engin.umich.edu

Coupled Alfvénic Turbulence in the Corona and the Solar Wind

- Electron-proton plasma
- Alfvénic turbulence wave energy densities

$$w_\pm = \tfrac{1}{2}\left[\tfrac{1}{2}\rho\,\langle\delta\mathbf{u}\cdot\delta\mathbf{u}\rangle + \frac{\langle\delta\mathbf{B}\cdot\delta\mathbf{B}\rangle}{2\mu_0}\right] + \sqrt{\frac{\rho}{\mu_0}}\,\langle\delta\mathbf{u}\cdot\delta\mathbf{B}\rangle\,; \qquad w_\mathrm{D} = \tfrac{1}{2}\rho\,\langle\delta\mathbf{u}\cdot\delta\mathbf{u}\rangle - \frac{\langle\delta\mathbf{B}\cdot\delta\mathbf{B}\rangle}{2\mu_0}$$

parallel/antiparallel
energy density

kinetic/magnetic
energy density difference

- Turbulence transport equations

reflection dissipation

$$\partial_t w_\pm + \boldsymbol{\nabla}\cdot(\mathbf{u}\,w_\pm \pm \mathbf{V}_\mathrm{A} w_\pm) + \tfrac{1}{2}w_\pm(\boldsymbol{\nabla}\cdot\mathbf{u}) + \tfrac{1}{2}(S \pm R)w_\mathrm{D} = -\Gamma_\pm w_\pm$$

$$\partial_t w_\mathrm{D} + \boldsymbol{\nabla}\cdot(w_\mathrm{D}\mathbf{u}) + \tfrac{1}{2}w_\mathrm{D}(\boldsymbol{\nabla}\cdot\mathbf{u}) + (S - R)w_+ + (S + R)w_- = \tfrac{1}{2}(\Gamma_+ + \Gamma_-)w_\mathrm{D}$$

reflection reflection dissipation

$$S = \tfrac{1}{2}\boldsymbol{\nabla}\cdot\mathbf{u} - \mathbf{b}\cdot(\mathbf{b}\cdot\boldsymbol{\nabla})\mathbf{u}; \qquad R = (\mathbf{b}\cdot\boldsymbol{\nabla})V_\mathrm{A}; \qquad \Gamma_\pm = \frac{2}{L_\perp}\sqrt{\frac{w_\mp}{\rho}}$$

- Correlation length scales with B$^{-1/2}$ in IH; it is more complicated in OH due to pickup ions

Acceleration and Heating of the Corona & Solar Wind

acceleration by wave pressure gradient

$$\partial_t(\rho\,\mathbf{u}) + \boldsymbol{\nabla}\cdot\left(\rho\mathbf{uu} - \frac{\mathbf{BB}}{\mu_0} - w_{\mathrm{D}}\mathbf{bb}\right) + \boldsymbol{\nabla}\left[p_i + p_e + \frac{B^2}{2\mu_0} \boxed{+ \tfrac{1}{2}(w_+ + w_- + w_{\mathrm{D}})}\right] = 0$$

$$\frac{1}{\gamma_{i/e}-1}\left[\partial_t p_{i/e} + \boldsymbol{\nabla}\cdot(p_{i/e}\mathbf{u})\right] + p_{i/e}(\boldsymbol{\nabla}\cdot\mathbf{u}) = \kappa_{i/e}\boxed{(\Gamma_+ w_+ + \Gamma_- w_-)}\,;\ \boxed{\kappa_i + \kappa_e = 1}$$

wave heating

dissipated wave energy partitioning

$$\partial_t\left(\tfrac{1}{2}\rho u^2 + \frac{1}{\gamma_i-1}p_i + \frac{1}{\gamma_e-1}p_e + \frac{B^2}{2\mu_0} + w_+ + w_-\right) +$$

$$\nabla\cdot\left[\left(\tfrac{1}{2}\rho u^2 + \frac{B^2}{\mu_0} + \frac{\gamma_i}{\gamma_i-1}p_i + \frac{\gamma_e}{\gamma_e-1}p_e + w_+ + w_-\right)\mathbf{u} + \overline{\overline{P}}_{\mathrm{A}}\cdot\mathbf{u} \boxed{+ (w_+ - w_-)\,\mathbf{V}_{\mathrm{A}}} - \frac{(\mathbf{u}\cdot\mathbf{B})}{\mu_0}\mathbf{B}\right] = 0$$

wave heating

$$\overline{\overline{P}}_{\mathrm{A}} = -w_{\mathrm{D}}\mathbf{bb} + \tfrac{1}{2}\left(w_+ + w_- + w_{\mathrm{D}}\right) I = \begin{bmatrix} \tfrac{1}{2}\rho\left\langle\delta\mathbf{u}\cdot\delta\mathbf{u}\right\rangle & 0 & 0 \\ 0 & \tfrac{1}{2}\rho\left\langle\delta\mathbf{u}\cdot\delta\mathbf{u}\right\rangle & 0 \\ 0 & 0 & \frac{1}{2\mu_0}\left\langle\delta\mathbf{B}\cdot\delta\mathbf{B}\right\rangle \end{bmatrix}$$

Maxwell stress tensor

Tamas I. Gombosi
tamas@umich.edu
https://tamas.engin.umich.edu

The Alfvén-Wave Solar Atmosphere Model (AWSoM)

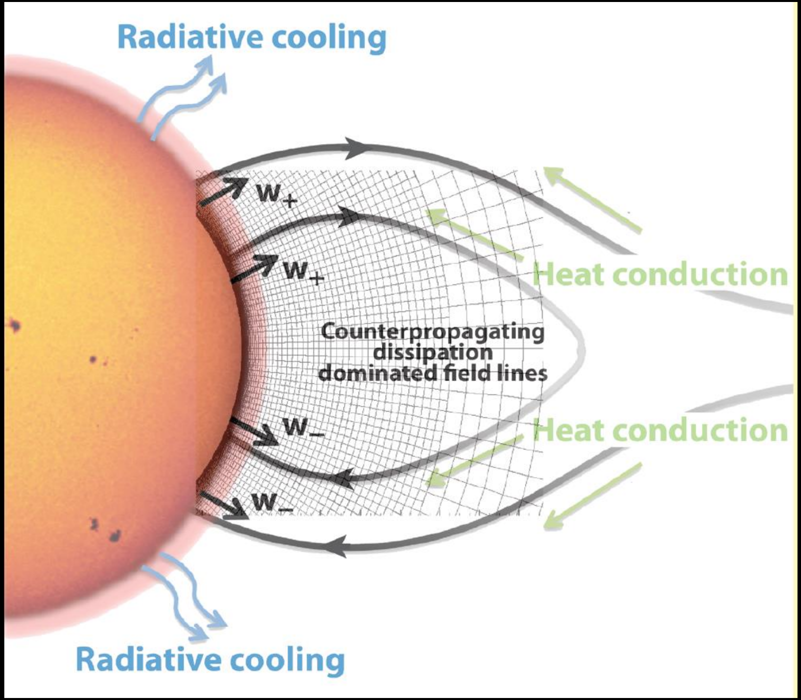

van der Holst+ 2014, doi: 10.1088/0004-637X/782/2/81
Sokolov+ 2021, doi: 10.3847/1538-4357/abc000

- Heat conduction:
  - Spitzer (r<5Rs)
  - Hollweg (r>5Rs)
- Radiative cooling from CHIANTI
- Wave pressure gradient accelerates and heats
- Two (T_i, T_e) or three ($T_{i||}$, $T_{i\perp}$, T_e) temperatures
- Turbulent energy transport along field lines

Tamas I. Gombosi
tamas@umich.edu
https://tamas.engin.umich.edu

Multiple Scales: XMHD with Adaptively Embedded PiC

- BATSRUS calculates physics criteria of reconnection from MHD quantities
- Use these criteria to find the reconnection sites
- Apply geometric criteria to restrict active PIC domain
- Expand active PIC grid around the reconnection sites
- Pass the information to PiC to adapt its grid

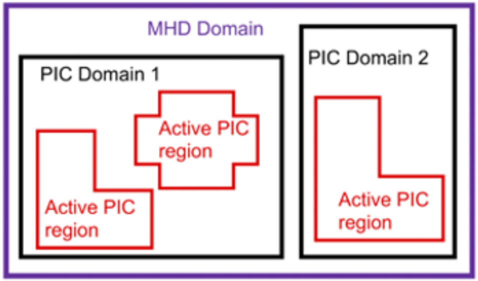

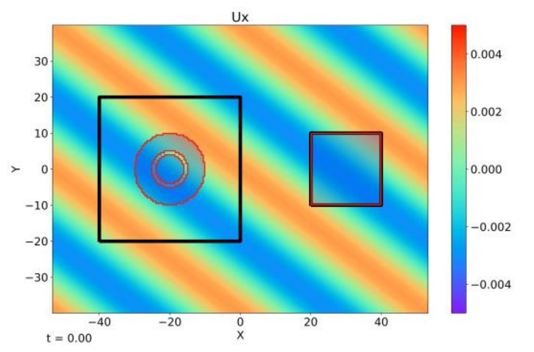

- PIC domains are black squares
- Active PIC regions are shadowed areas, enclosed by red lines

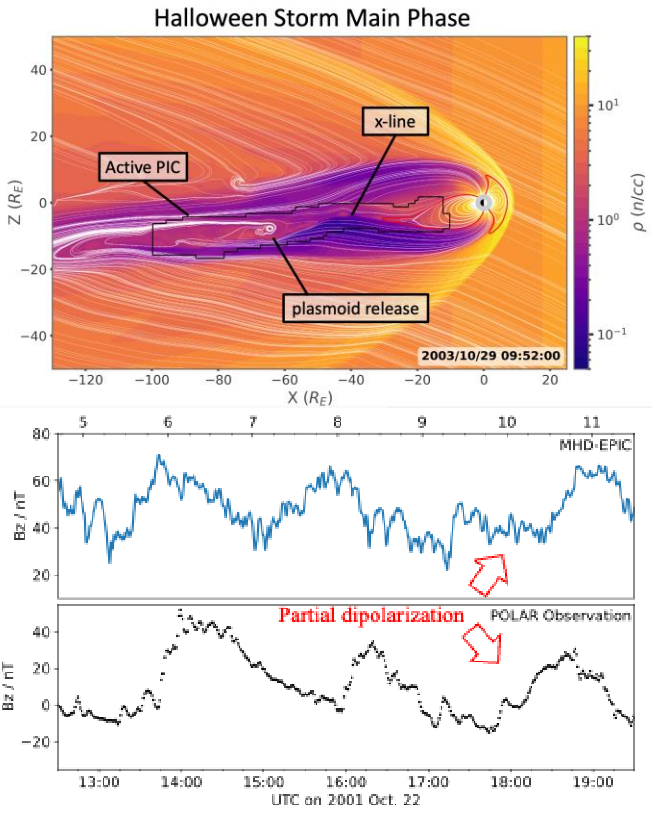

Wang et al, GRL 2022

SWMF in 2024

SWMF is open-source at
http://github.com/SWMFsoftware
and also available via CCMC

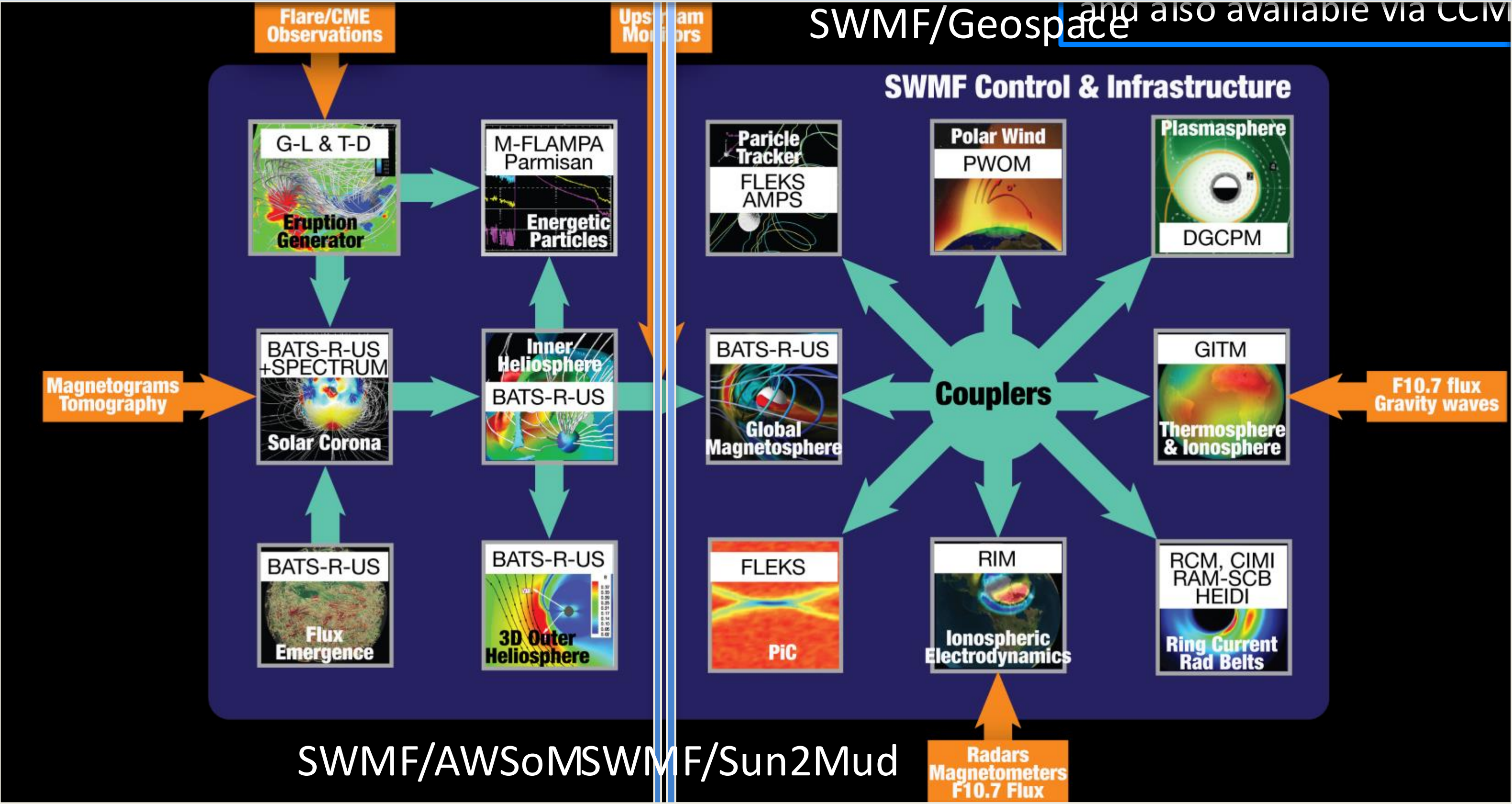

SWMF/Geospace

SWMF/AWSoM

SWMF/Sun2Mud

Tamas I. Gombosi
tamas@umich.edu
https://tamas.engin.umich.edu

2024 SWMF/BATS-R-US Code Summary

- Source code (active = tested): 1.3M lines
  - 692K lines of Fortran with MPI + OpenMP parallelization
  - 330K lines of C++
  - 246K lines of scripts, makefiles and XML descriptions
  - 26K lines of wrappers and couplers
- SWMF runs on Unix/Linux/OSX/WSL systems with Fortran 2008, C++, Perl, Python compilers/interpreters and optional MPI, OpenMP, OpenACC, AMREX, HYPRE, HDF5 libraries.
- The SWMF can run on a laptop or on tens of thousands of processors.
- Extensive user manual with up-to-date documentation of input parameters.
- Fully automated nightly testing with several machine/compiler combinations. These tests provide working examples for applications.

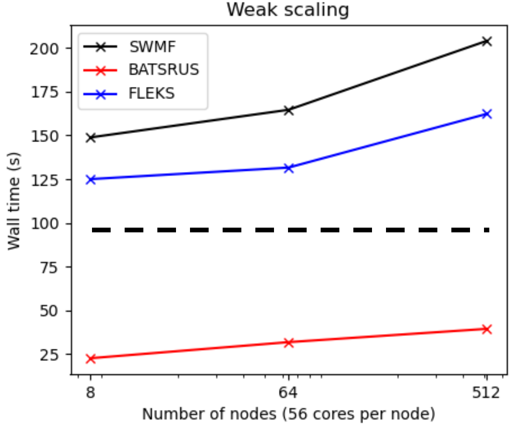

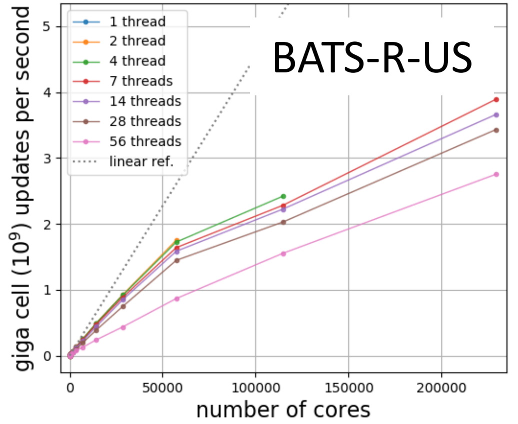

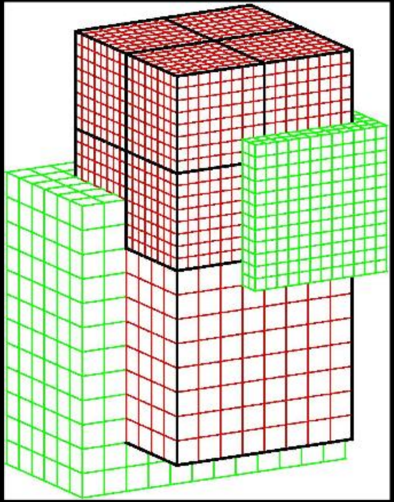

Block AMR

Tamas I. Gombosi
tamas@umich.edu
https://tamas.engin.umich.edu

The Space Weather Modeling Framework (SWMF)

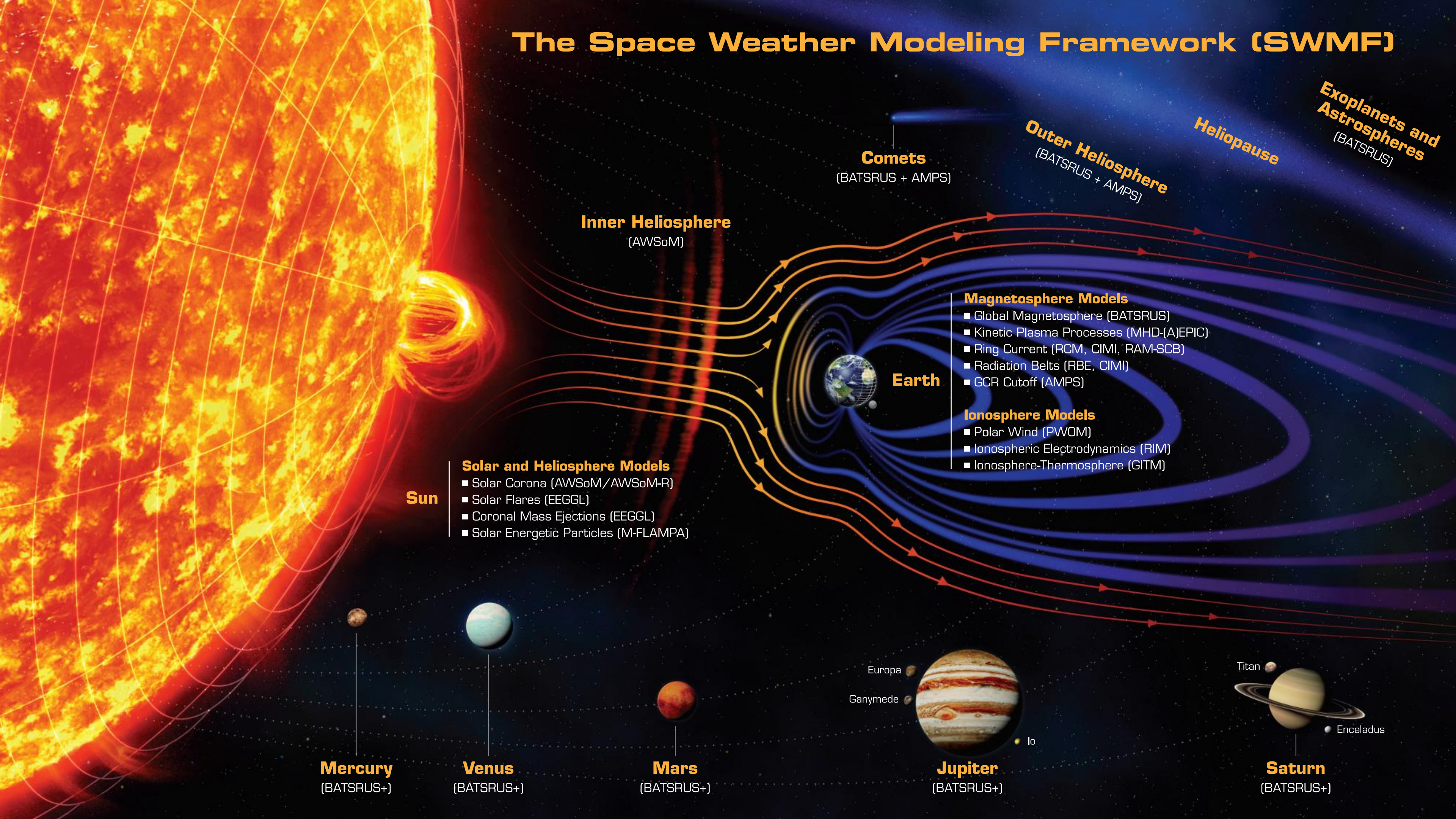

Comets
(BATSRUS + AMPS)

Outer Heliosphere
(BATSRUS + AMPS)

Heliopause

Exoplanets and Astrospheres
(BATSRUS)

Inner Heliosphere
(AWSoM)

Earth

Magnetosphere Models
- Global Magnetosphere (BATSRUS)
- Kinetic Plasma Processes (MHD-(A)EPIC)
- Ring Current (RCM, CIMI, RAM-SCB)
- Radiation Belts (RBE, CIMI)
- GCR Cutoff (AMPS)

Ionosphere Models
- Polar Wind (PWOM)
- Ionospheric Electrodynamics (RIM)
- Ionosphere-Thermosphere (GITM)

Sun

Solar and Heliosphere Models
- Solar Corona (AWSoM/AWSoM-R)
- Solar Flares (EEGGL)
- Coronal Mass Ejections (EEGGL)
- Solar Energetic Particles (M-FLAMPA)

Mercury
(BATSRUS+)

Venus
(BATSRUS+)

Mars
(BATSRUS+)

Jupiter
(BATSRUS+)

Saturn
(BATSRUS+)

SWMF in Operational Use: SWMF/Geospace

- January 2012:
  - On behalf of NOAA/SWPC, the CCMC starts evaluation of Geospace prediction models to determine which model or models should begin transition to operations
  - Focus is on identifying models that can predict regional geomagnetic activity with useful skill scores
- November 2013:
  - Based on the results of two CCMC reports (one on dB/dt and the other on Regional K), as well as information learned throughout this process from numerous meetings and forums and one-on-one discussions with modelers and the CCMC, NOAA/SWPC decides to transition the University of Michigan’s Space Weather Modeling Framework (SWMF) to operations

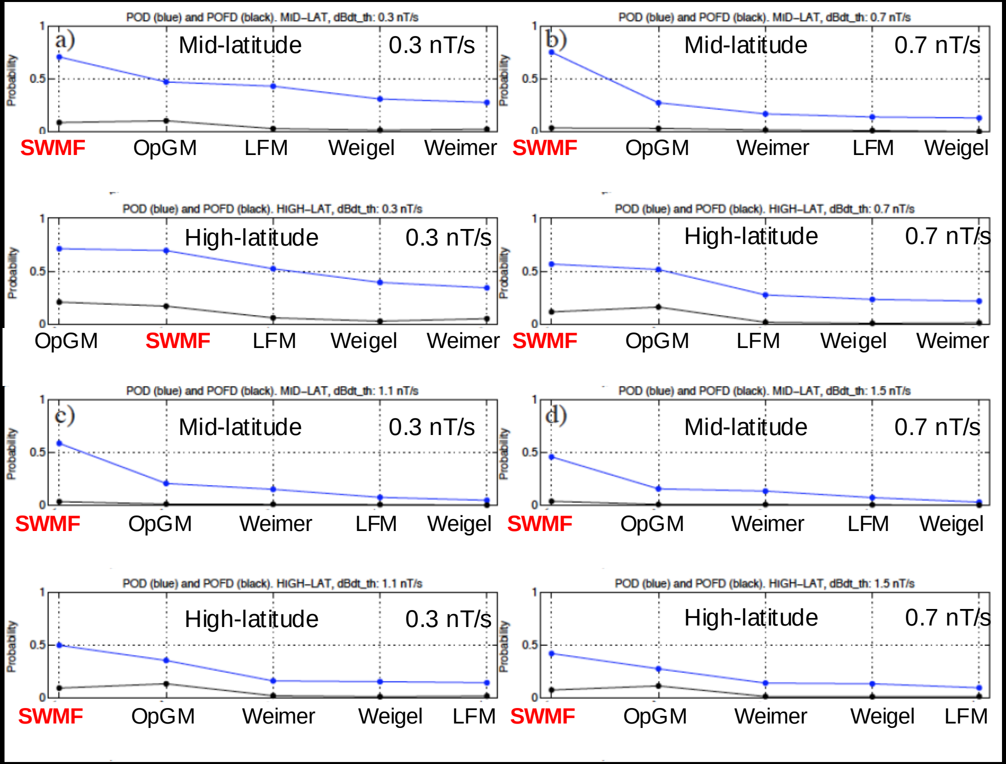

Tamas I. Gombosi
tamas@umich.edu
https://tamas.engin.umich.edu

SWMF/Geospace Operational Forecast: 2024 Mothers Day Event

GEOSPACE GEOMAGNETIC ACTIVITY PLOT **2024-05-11 03:37 UTC** **delta B [nT]**

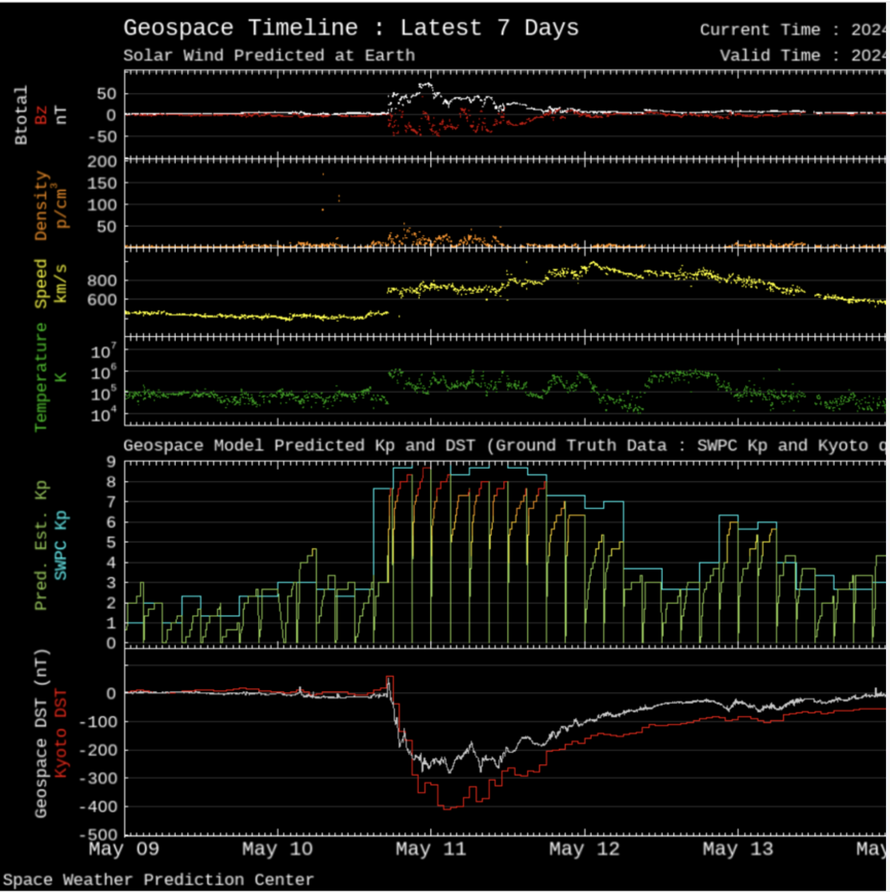

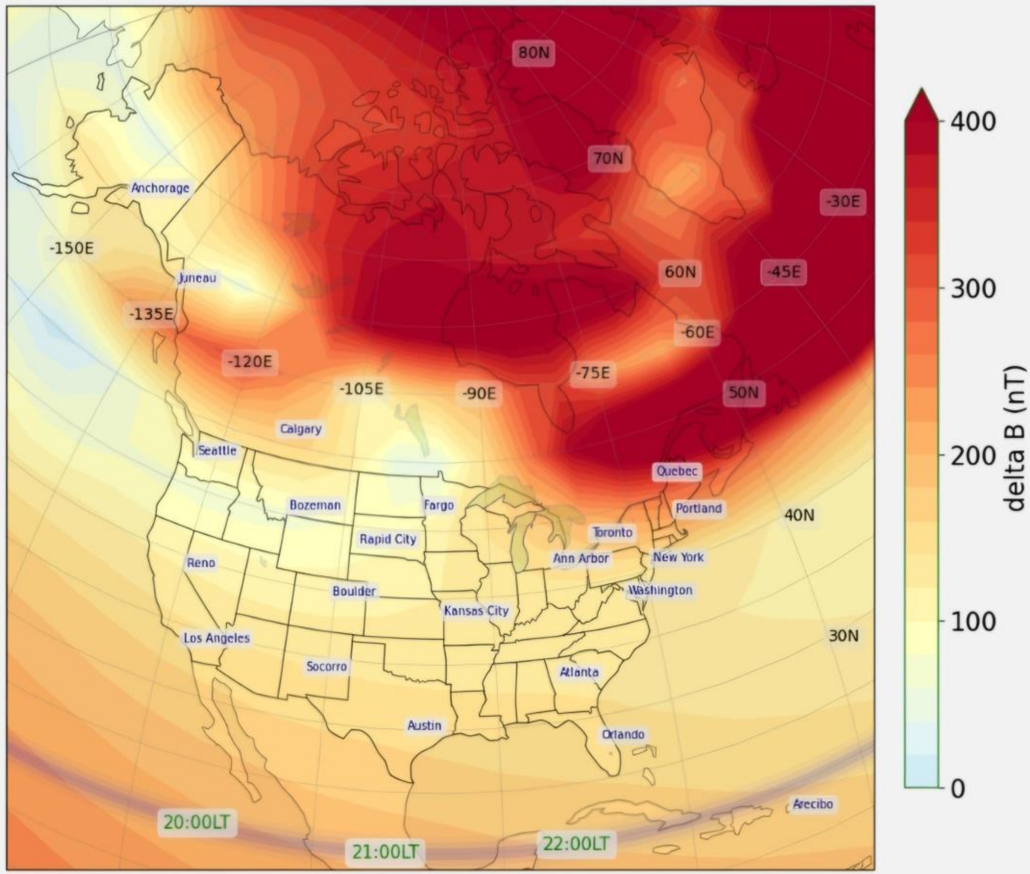

Resolving Mesoscale Features with AMR

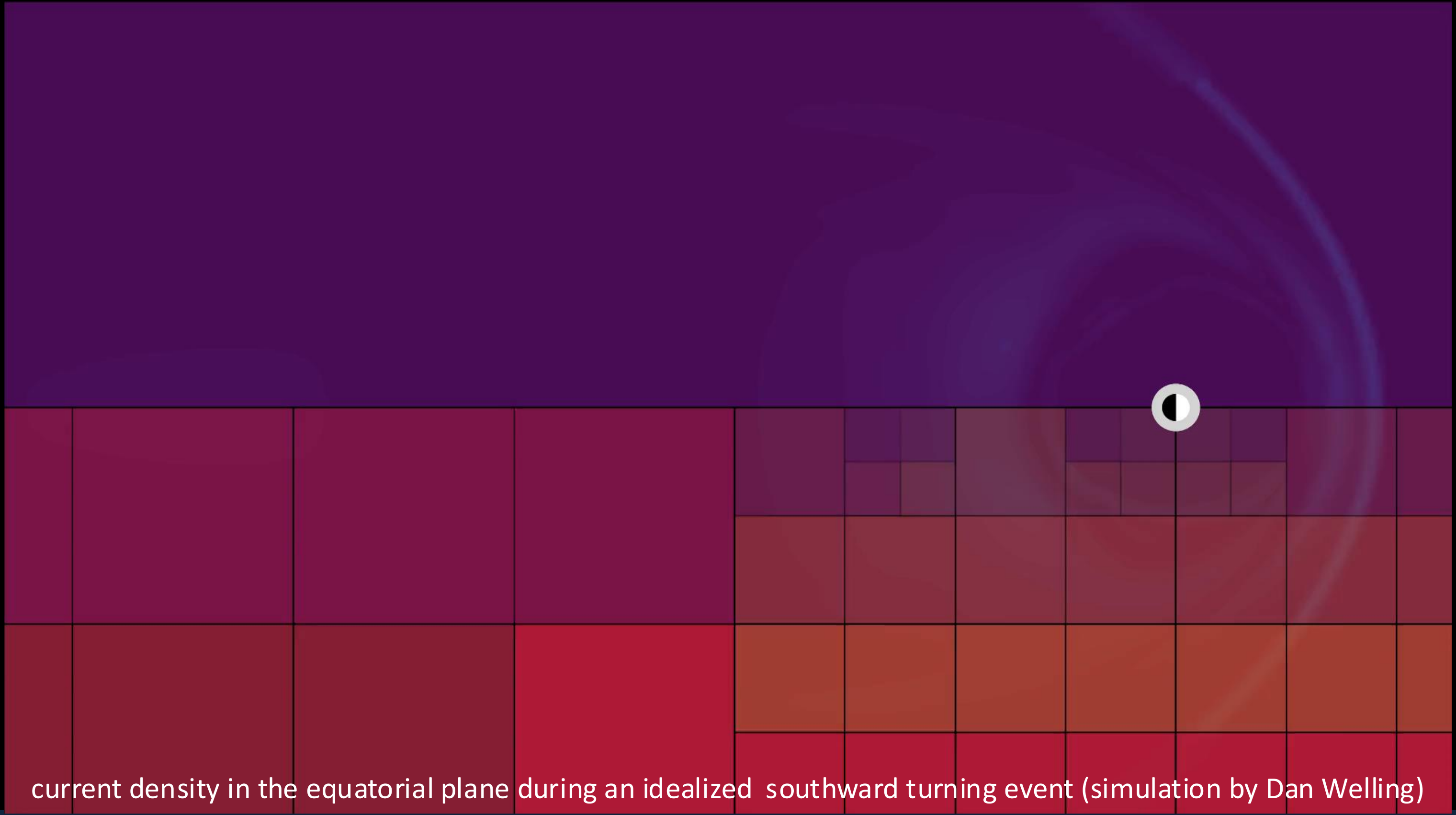

current density in the equatorial plane during an idealized southward turning event (simulation by Dan Welling)

Energy Flow in the Magnetosphere

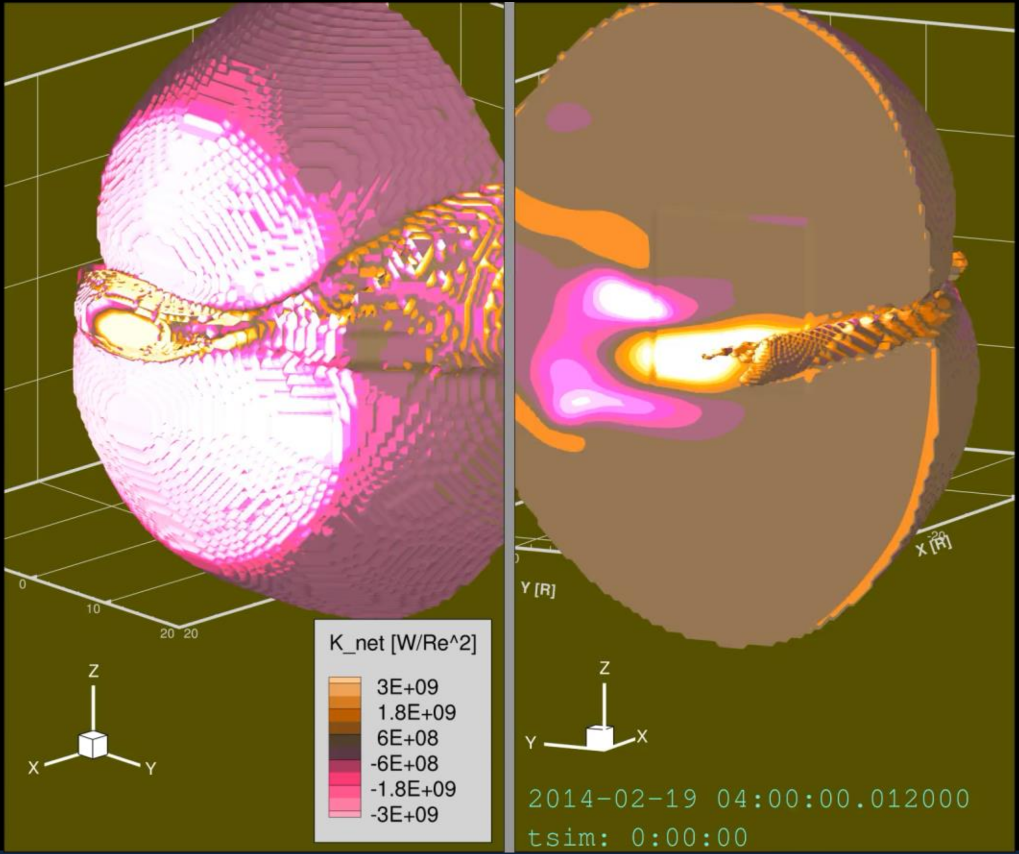

(simulation by Austin Brenner)

Resolving Electron Scale Features with MHD-EPIC

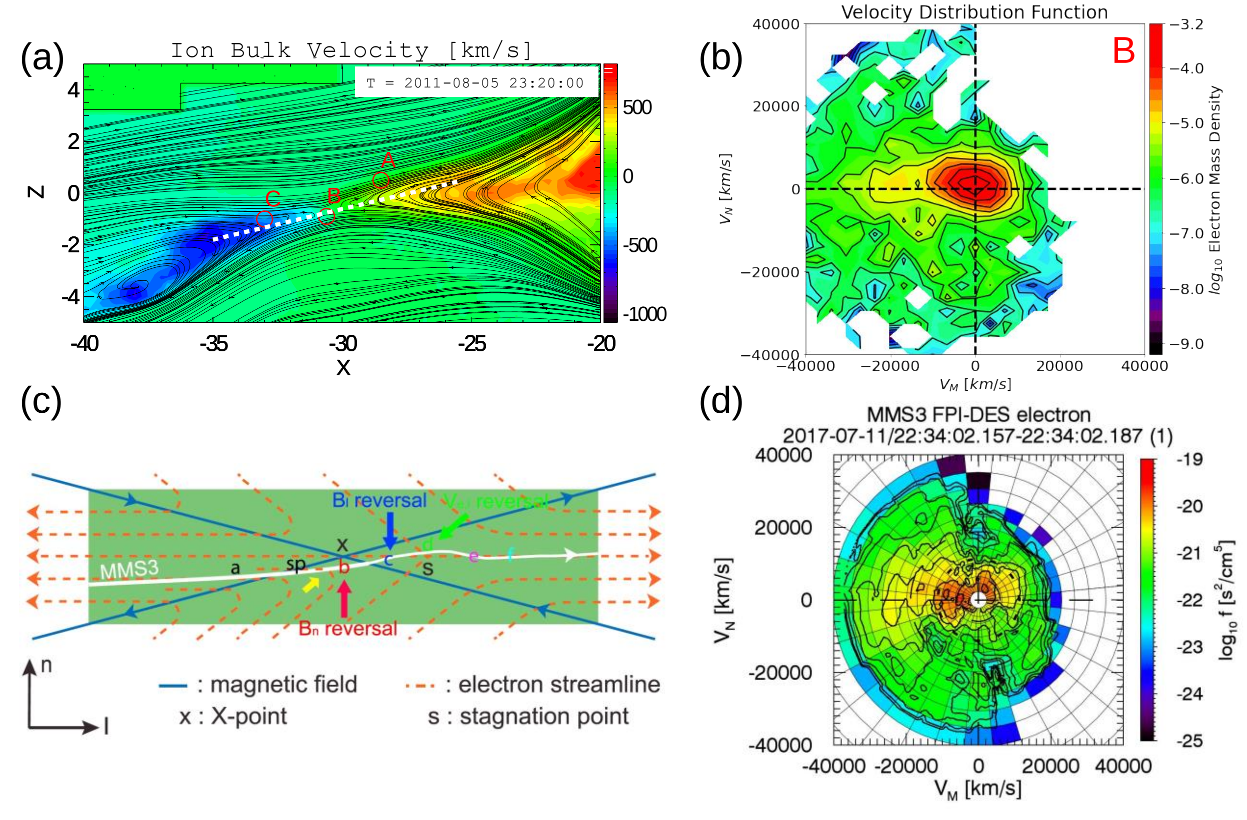

Wang et al., JGR, 2022

Tamas I. Gombosi
tamas@umich.edu
https://tamas.engin.umich.edu

Simulating the Background Corona and Solar Wind

- In the chromosphere the solar plasma transitions from high β (gas dominated) to low β (magnetic field dominated) regime
- In the narrow ($>10^2$ km) transition region heat conduction from the corona is balanced by radiative cooling
- There is growing consensus that Alfvénic turbulence is primarily responsible for accelerating and heating the solar wind
- Data driven corona/solar wind models use photospheric magnetic field measurements to derive boundary conditions in the low transition region
- The new generation of models (will) use time evolving vector magnetic field maps
- A big unknown is the connection between the photospheric and transition region magnetic fields

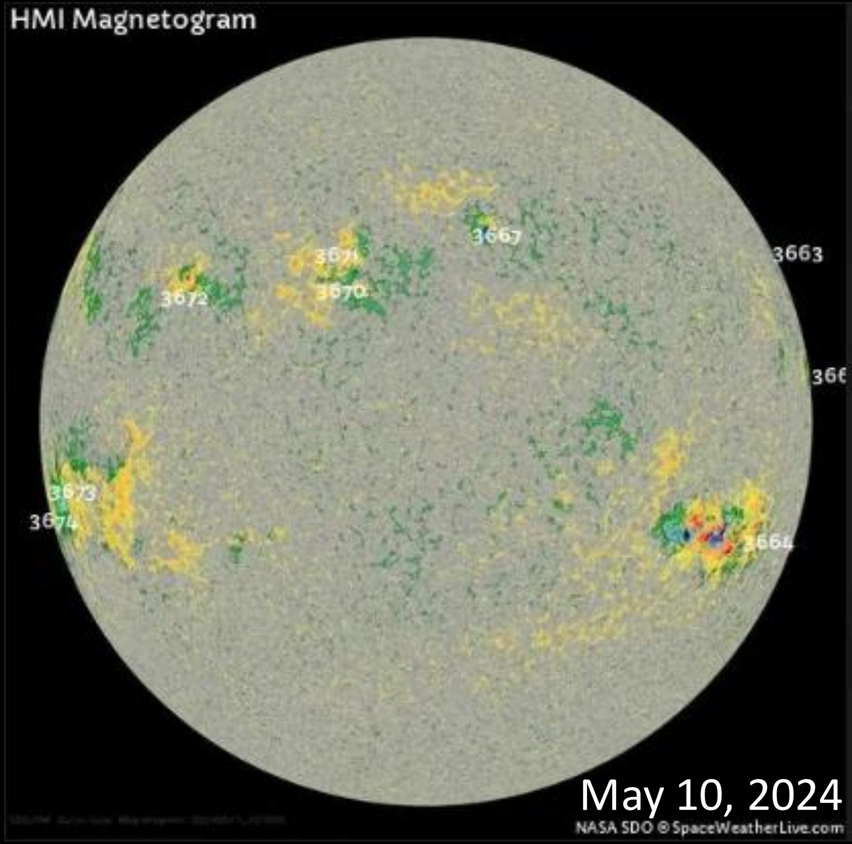

May 10, 2024

NASA SDO © SpaceWeatherLive.com

Tamas I. Gombosi
tamas@umich.edu
https://tamas.engin.umich.edu

Solar Wind and Magnetic Connectivity

- Magnetic connectivity in the heliosphere is a critical information for
    - Identifying solar wind source regions on the Sun
    - interpreting energetic particle observations in the heliosphere
- In (near-)ideal MHD, IMF field lines and plasma streamlines are parallel/antiparallel beyond the Alfvén point
- In numerical simulations
    - unavoidable numerical reconnection for field lines near the HCR lead to false connectivity (v-shaped IMF)…

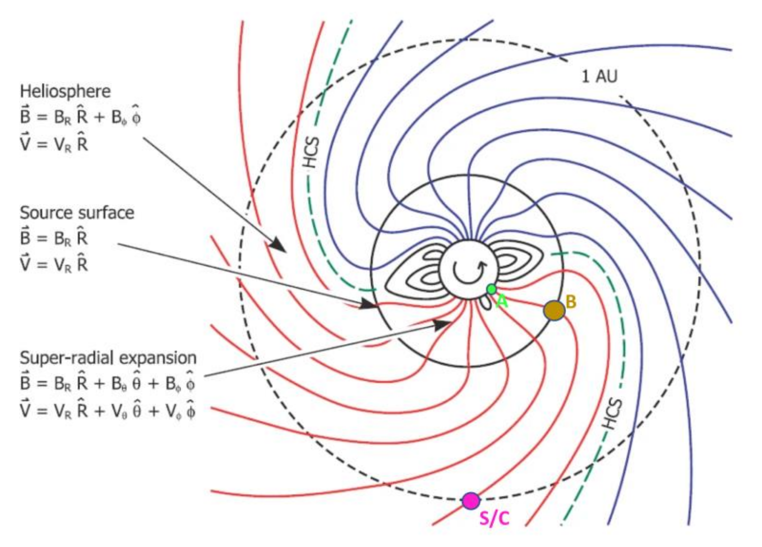

Owens, M.J. and Forsyth, R.J., *Living Rev. Sol. Phys.* **10**, 5 (2013). https://doi.org/10.12942/lrsp-2013-5

IMF Lines Reconnect Near Current Sheets

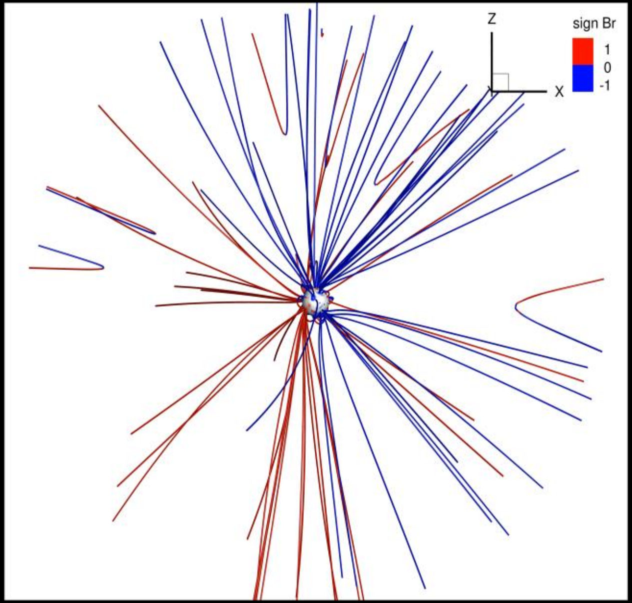

AWSoM

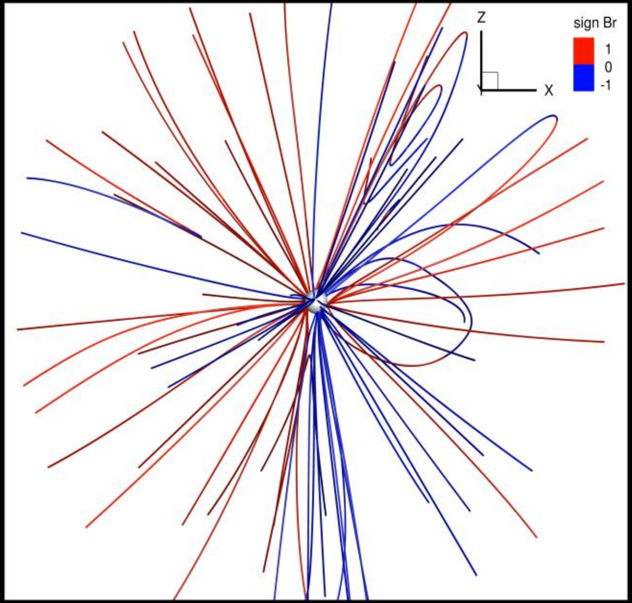

MAS

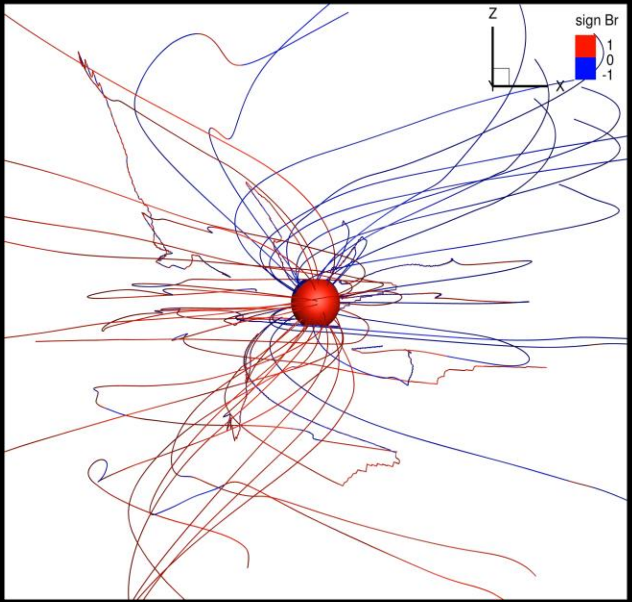

ENLIL

Stream-Aligned MHD

Sokolov et al. (2022), ApJ, 926, 102,
doi: 10.3847/15384357/ac400f

- In the free streaming solar wind we expect the **u** and **B** vectors to be parallel everywhere: $\mathbf{B} = \alpha(t,\mathbf{r})\,\mathbf{u}$
- $\alpha(t,\mathbf{r})$ is a scalar function
- Obviously, $\mathbf{E}=-\mathbf{u}\times\mathbf{B}\equiv 0$
- It can be shown that $\partial_t\alpha = -\nabla\cdot(\alpha\mathbf{u})$
- Aligning force: $\alpha\partial_t\mathbf{u} = -\nabla\cdot(\alpha\mathbf{u})$. As steady-state is approached, $\alpha\partial_t\mathbf{u} \Rightarrow 0$
- Add the aligning force to the induction and momentum equations:

$$\partial_t\mathbf{B} + \nabla\cdot(\mathbf{uB}-\mathbf{Bu}) = -\mathbf{u}(\nabla\cdot\mathbf{B}) + \alpha\partial_t\mathbf{u}$$

$$\partial_t\mathbf{u} + (\mathbf{u}\cdot\nabla)\mathbf{u} + \frac{\nabla P}{\rho} = \frac{\alpha}{\mu_0\rho}[\nabla\times(\alpha\mathbf{u})]\times\mathbf{u}$$

$$\partial_t\left(\frac{\rho u^2}{2}+\frac{P}{\gamma-1}\right)+\nabla\cdot\left[\left(\frac{\rho u^2}{2}+\frac{\gamma P}{\gamma-1}\right)\mathbf{u}\right]=0$$

- Aligning force is ⊥ to the velocity and it does not affect the kinetic energy, hence, does not exchange energy between the field and plasma
- This model is valid for steady-state in the corotating frame

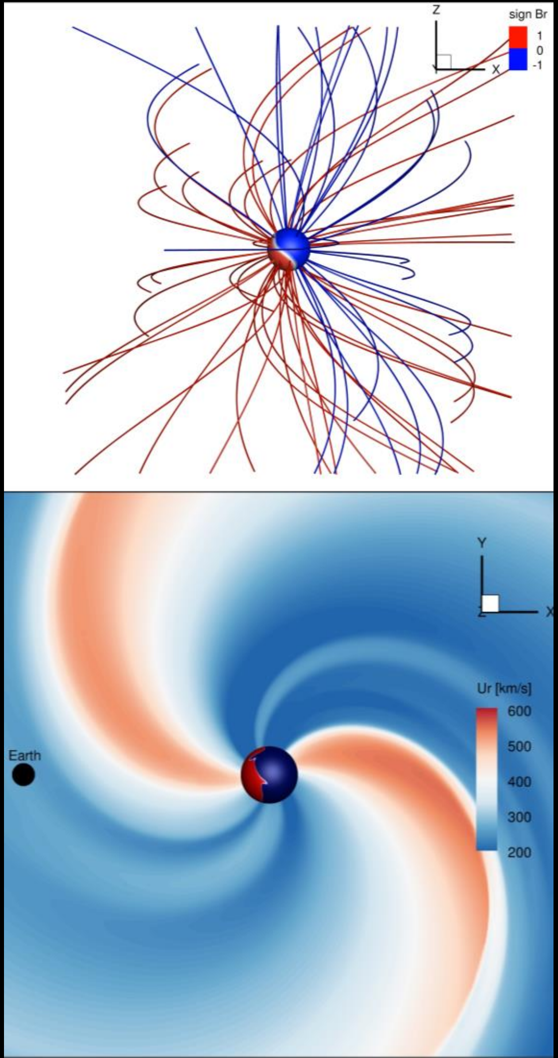

Background Corona/Solar Wind Simulations

Sachdeva et al. 2023, ApJ
doi: 10.3847/1538-4357/acda87

CR 2107 (ascending phase)

AWSoM

SDO/AIA

AWSoM

SDO/AIA

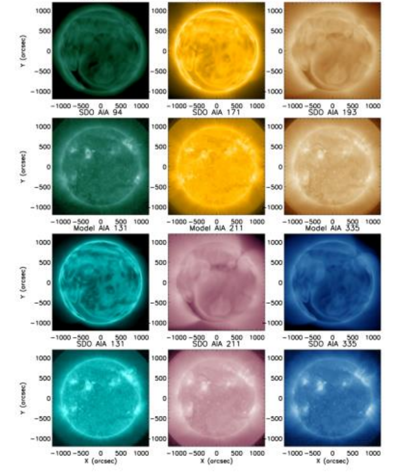

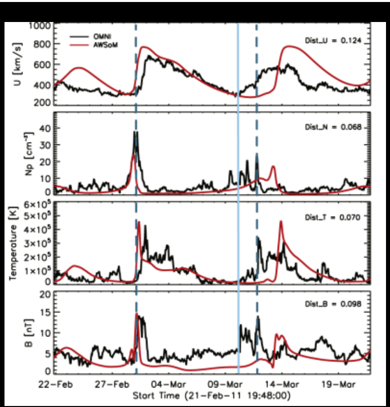

CR 2123 (solar max)

AWSoM

SDO/AIA

AWSoM

SDO/AIA

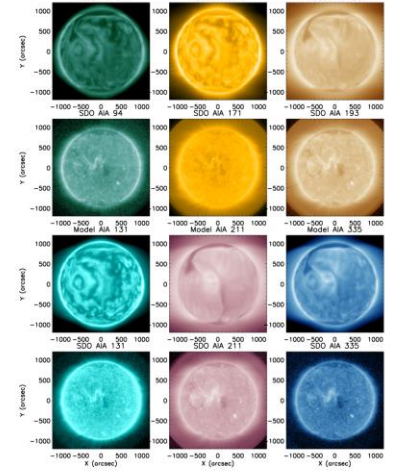

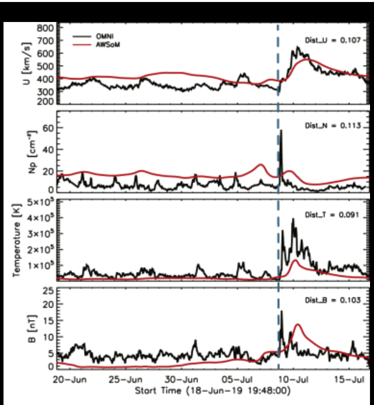

CR 2219 (solar min)

AWSoM

SDO/AIA

AWSoM

SDO/AIA

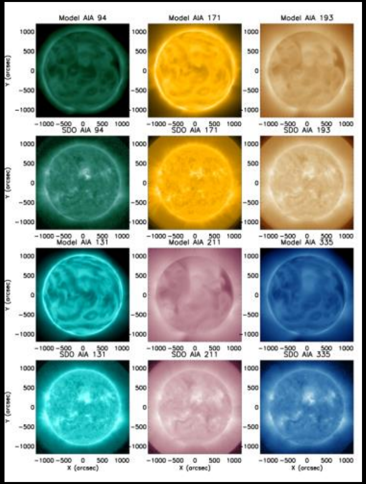

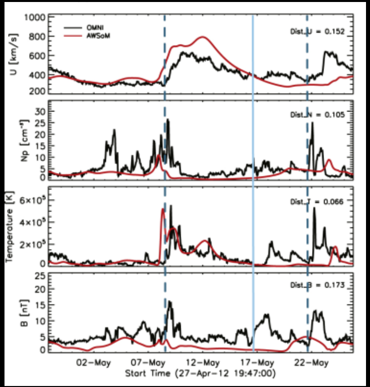

CME Initiation

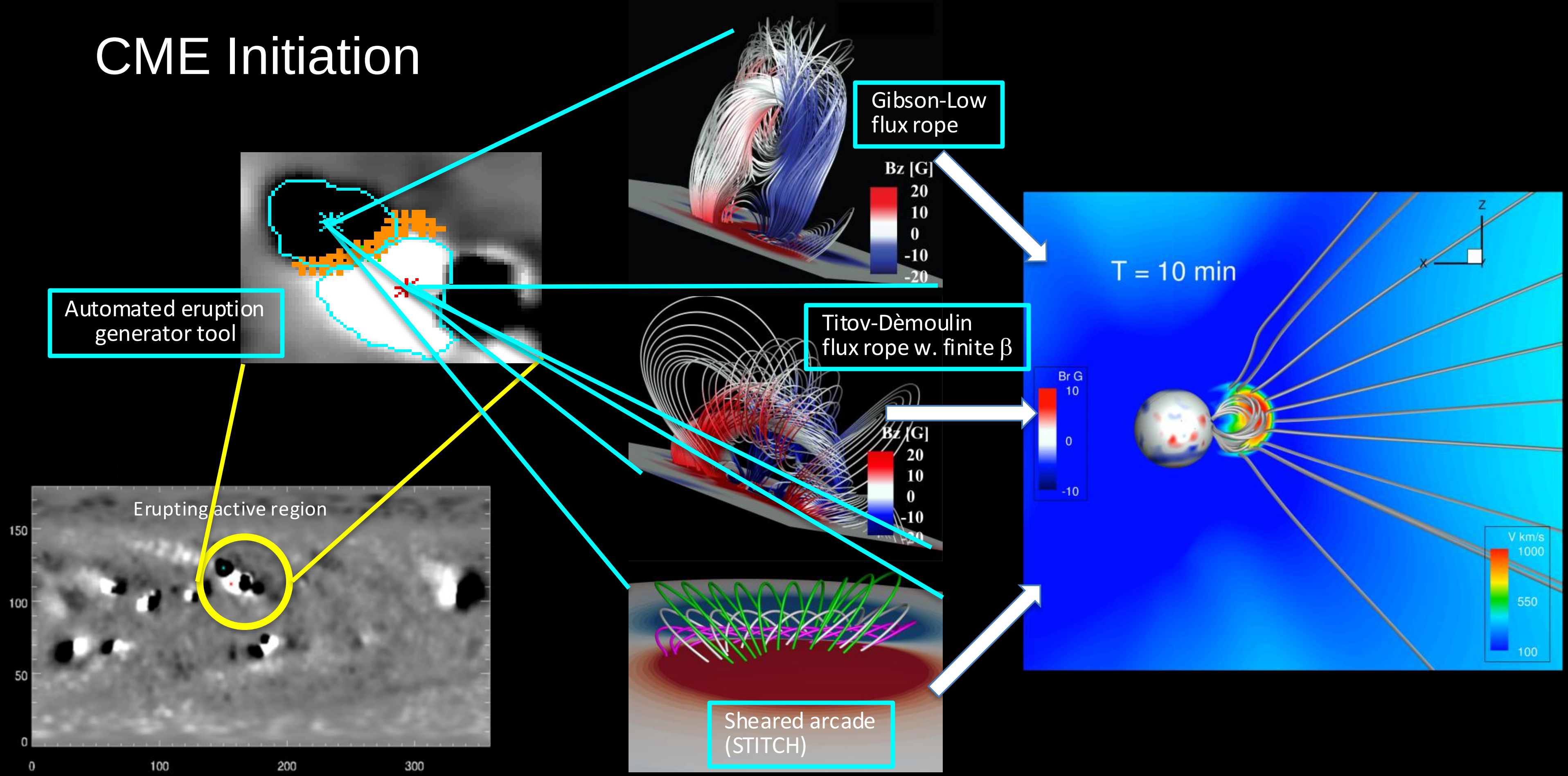

Gibson-Low flux rope

Titov-Dèmoulin flux rope w. finite β

Sheared arcade (STITCH)

Automated eruption generator tool

Erupting active region

M-FLAMPA: Lagrangian Multiple IMF-Line Tracker

- Extract IMF lines from any MHD snapshot of the heliosphere

$$\{x,y,z\}_{new} = \{x,y,z\}_{old} + \Delta s \frac{\mathbf{B}\left(\{x,y,z\}_{old}\right)}{B\left(\{x,y,z\}_{old}\right)}$$

- In an inertial frame, field lines and stream-lines are the same (except for reconnection)

$$\{x,y,z\}_{new} = \{x,y,z\}_{old} + \Delta t \frac{\mathbf{u}\left(\{x,y,z\}_{old}\right)}{u\left(\{x,y,z\}_{old}\right)}$$

- Once a field line is extracted its time evolution can be obtained

$$\{x,y,z\}_{new} = \{x,y,z\}_{old} + \Delta t\, \mathbf{u}\left(\{x,y,z\}_{old}\right)$$

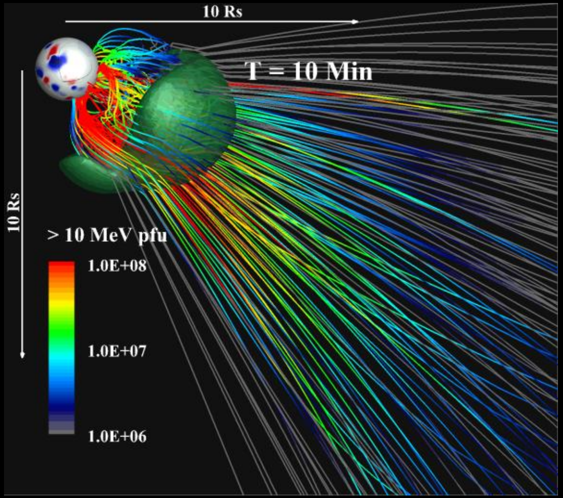

Sokolov et al. (2004), ApJ, doi: 10.1086/426812
Borovikov et al. (2018), ApJ, doi: 10.3847/1538-4357/aad68d

SEP Simulations: AWSoM + M-FLAMPA + PARMISAN

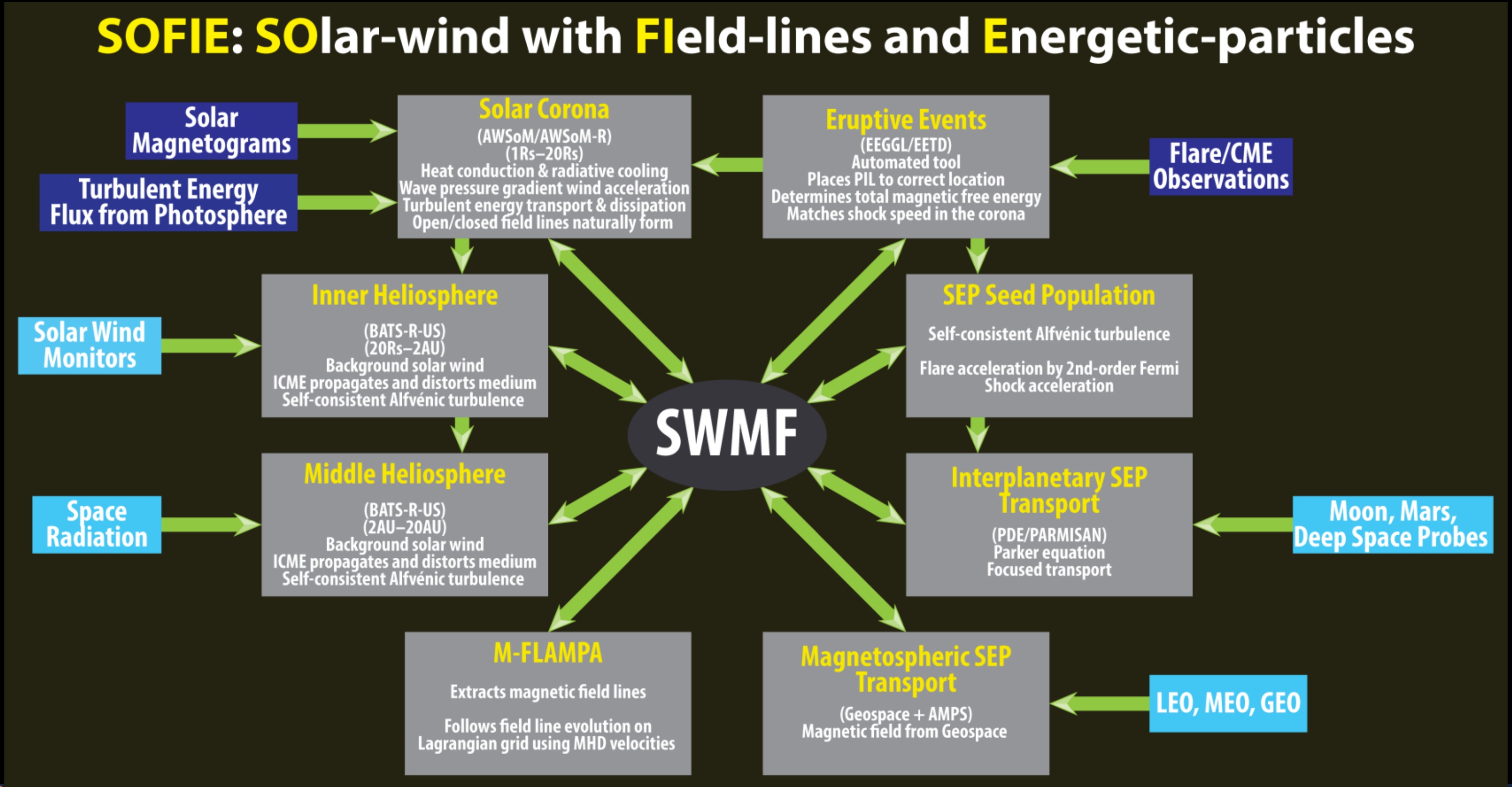

SOFIE: SOlar-wind with FIeld-lines and Energetic-particles

Solar Magnetograms

Turbulent Energy Flux from Photosphere

Solar Corona
(AWSoM/AWSoM-R)
(1Rs–20Rs)
Heat conduction & radiative cooling
Wave pressure gradient wind acceleration
Turbulent energy transport & dissipation
Open/closed field lines naturally form

Eruptive Events
(EEGGL/EETD)
Automated tool
Places PIL to correct location
Determines total magnetic free energy
Matches shock speed in the corona

Flare/CME Observations

Solar Wind Monitors

Inner Heliosphere
(BATS-R-US)
(20Rs–2AU)
Background solar wind
ICME propagates and distorts medium
Self-consistent Alfvénic turbulence

SWMF

SEP Seed Population
Self-consistent Alfvénic turbulence

Flare acceleration by 2nd-order Fermi
Shock acceleration

Space Radiation

Middle Heliosphere
(BATS-R-US)
(2AU–20AU)
Background solar wind
ICME propagates and distorts medium
Self-consistent Alfvénic turbulence

Interplanetary SEP Transport
(PDE/PARMISAN)
Parker equation
Focused transport

Moon, Mars, Deep Space Probes

M-FLAMPA
Extracts magnetic field lines

Follows field line evolution on
Lagrangian grid using MHD velocities

Magnetospheric SEP Transport
(Geospace + AMPS)
Magnetic field from Geospace

LEO, MEO, GEO

Tamas I. Gombosi
tamas@umich.edu
https://tamas.engin.umich.edu

SOFIE: Integrated Solar Wind + CME + SEP Simulation Tool

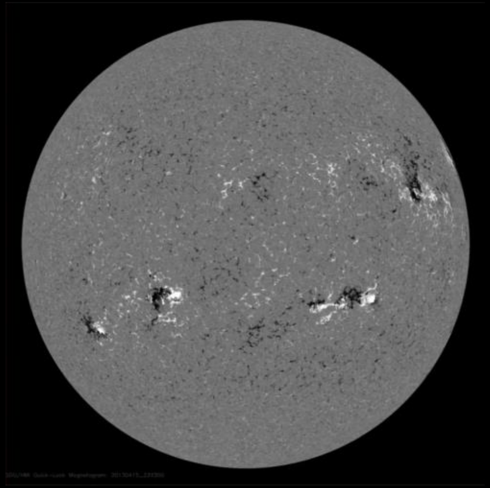

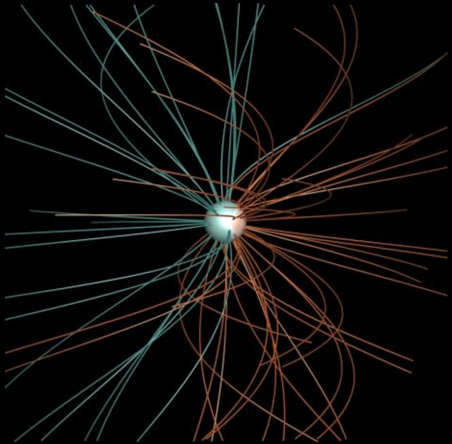

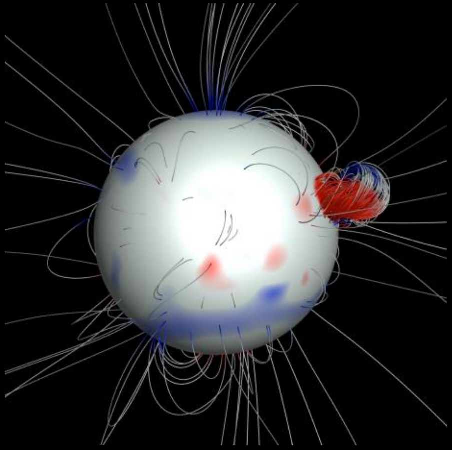

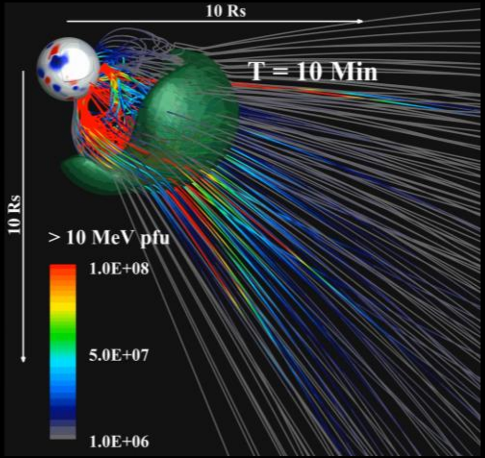

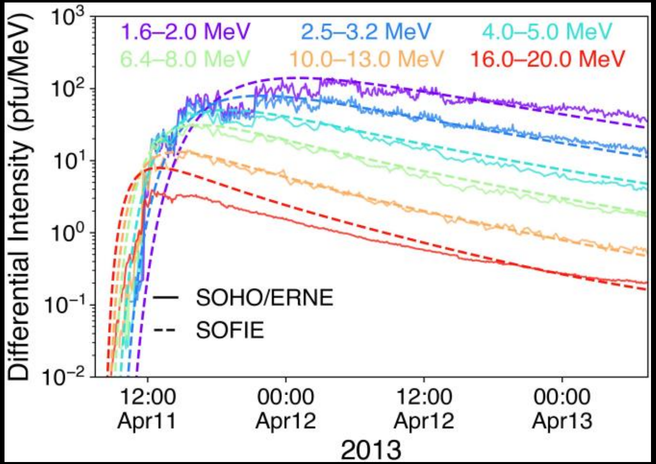

Summary

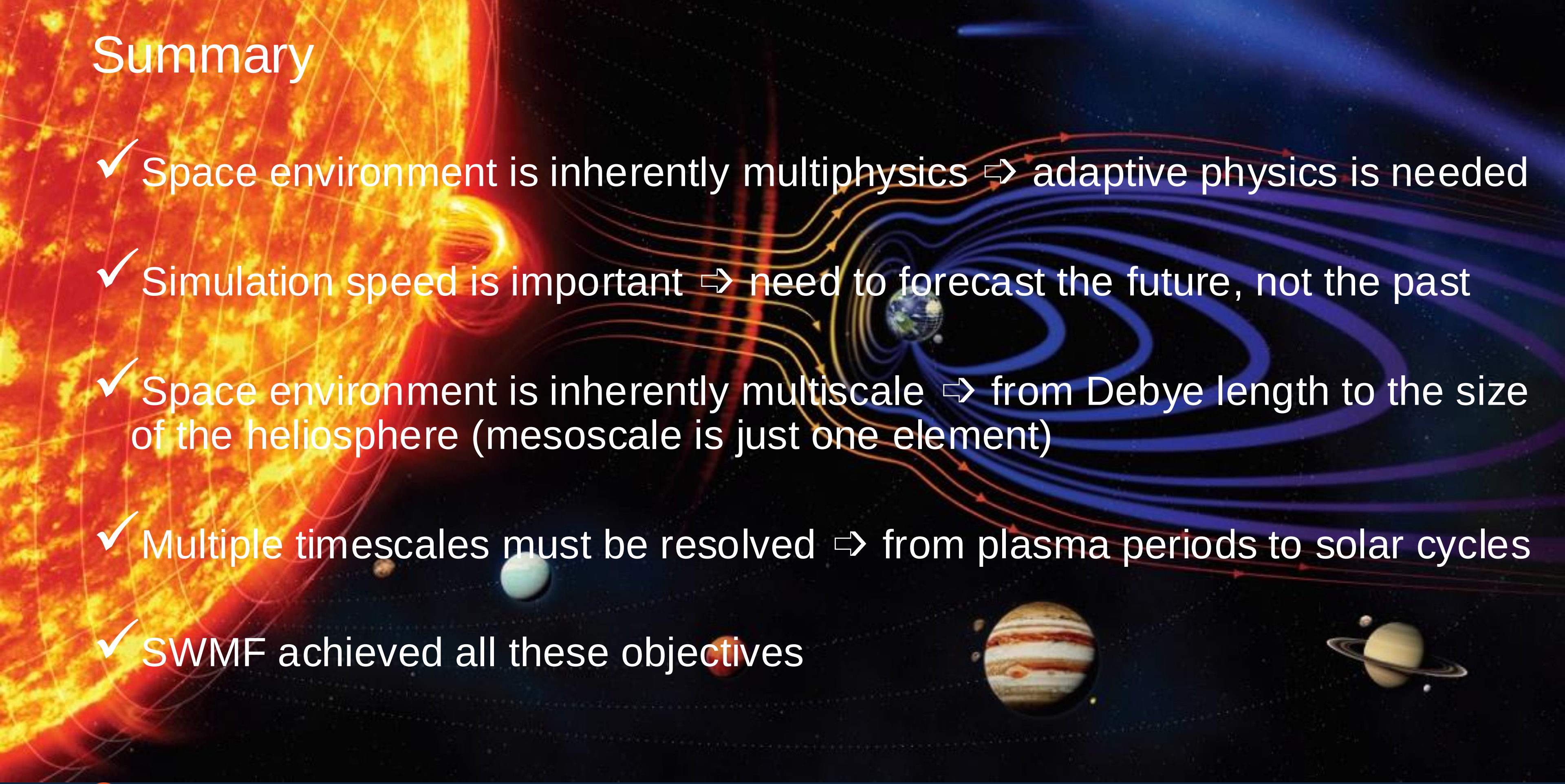

- ✓ Space environment is inherently multiphysics ⇨ adaptive physics is needed
- ✓ Simulation speed is important ⇨ need to forecast the future, not the past
- ✓ Space environment is inherently multiscale ⇨ from Debye length to the size of the heliosphere (mesoscale is just one element)
- ✓ Multiple timescales must be resolved ⇨ from plasma periods to solar cycles
- ✓ SWMF achieved all these objectives

Tamas I. Gombosi
tamas@umich.edu
https://tamas.engin.umich.edu